

Effect of the interactions between crystal and gel hydration products on the volume change of cementitious materials

Depeng Zhang[a], Hui Li[a], Zhenyu Pi[a], Mingfeng Xu[a], Jian Zhou[a,*], Mingzhong Zhang[b]

a. School of Civil and Transportation Engineering, Hebei University of Technology, Tianjin 300401, China

b. Department of Civil, Environmental and Geomatic Engineering, University College London, London WC1E 6BT, UK

*. Corresponding author: zhoujian@hebut.edu.cn

Effect of the interactions between crystal and gel hydration products on the volume change of cementitious materials

Abstract:

The volume change of cementitious materials is often studied based on the properties of the individual hydration product, either from the gel products causing shrinkage or the crystal products causing expansion. Previous studies of the team have theoretically revealed that the interactions between crystal and gel products produce the "micro self-stressing", which affects the volume change of cementitious materials. This work presents theoretical and experimental studies into the impact of the interactions between crystal and gel products on the volume change of cementitious materials. Firstly, a theoretical model for the volume change of cementitious materials was proposed. Secondly, in the followed experiment, the crystallization pressure, which affects the interactions between crystal and gel products, was tailored by immersing specimens in different exchange solvents or solutions to change the solubility product. Water, isopropyl alcohol, ethanol, calcium hydroxide and calcium acetate were selected as the exchange solvents or solutions. Subsequently, cement pastes were vacuum dried. Volume changes of cement pastes were tested during the whole process. Inductively-coupled plasma mass spectrometry and ion chromatography were utilized to test the ion concentrations and calculate the crystallization pressure. Finally, the experimental results were compared with the calculated results to validate the model. Results indicated that cement pastes immersed in different solvents or solutions exhibited different volume changes. An increase in crystallization pressure by 45.3% resulted in a 46.1% increase in the expansion of cement paste. Moreover, the reduction in the interactions should be one of the factors contributing to the drying shrinkage of cement paste.

Keywords: Cementitious materials, Expansion, Shrinkage, Crystallization pressure, Hydration products

1. Introduction

Concrete typically undergoes macroscopic volume changes due to the gain or loss of water, which can lead to cracking, altered mechanical properties and reduced structural durability, ultimately affecting the overall engineering quality. The volume change component in concrete is the cement paste [1,2]. The cement paste is mainly composed of hydration products and unhydrated cement particles. The spatiotemporal evolution of hydration products significantly affects the performance of cement paste.

Cement pastes exhibit varying volume changes behaviors under different environmental conditions, including shrinkage in dry environments and expansion in wet conditions [3]. Three primary mechanisms contribute to the drying shrinkage of Portland cement paste: the solid surface free energy [4–7], capillary forces [5,8–10], and disjoining pressure [5,11–14]. It is reported that the shrinkage of cement paste is caused by the combined effects of the above mechanisms [15]. More recently, an analytical framework by multi-mechanism approach based on above three mechanisms was established, and a drying shrinkage formulation was adopted [14]. However, the shrinkage caused by those mechanisms cannot fully describe the total drying shrinkage of cement paste [14].

The expansion mechanism of cement paste can be explained by three theories: water adsorption [3], increase in solid volume [16,17], and crystallization pressure. However, calcium sulfoaluminate (CSA) cement, whose hydration products are mainly ettringite (AFt) or monosulfoaluminate (AFm) crystals that cannot adsorb many water molecules, exhibits greater expansion [18,19]. Thus, water adsorption should not be the primary cause of this expansion. In addition, no direct relationship was observed between the volume of ettringite formed and the expansion of the cement paste in CSA expansive cement [20], suggesting that the increase in solid volume should not be the primary cause of expansion. Crystals growing in a supersaturated solution can exert sufficient force to lift a specific mass [21]. This phenomenon is attributed to the development of the crystallization pressure. The theory of crystallization pressure appears to be the most plausible explanation for the observed expansion of the cement paste [17,22–24].

The growth of crystal is controlled by the interface attachment kinetics [25]. Crystallization pressure is generated when a crystal grows within a confined space such as a grain boundary or contact area, exerting pressure on the surrounding material [26]. Crystallization pressure is generated when a thin fluid layer exists at the crystal-solid interface [27], but disappears when the thin fluid layer is gone [28]. The reason is that the fluid layer provides a mass transport channel for the growing crystal. With crystallization pressure, the crystal continues to grow or exert greater stress on the surrounding materials until the chemical potential at the interface reaches equilibrium with that in the solution. It is a process in which chemical potential is converted into mechanical work.

Crystallization pressure in cementitious materials often leads to changes in the properties of the matrix. It has been reported that the crystallization pressure in pores can generate a tensile pressure, and the matrix cracks when this pressure exceeds the tensile strength of the samples [29,30]. A model based on the crystallization pressure with a single pore was established to calculate the average hydrostatic tensile stress in the solid, and it showed that the expansion is affected by the temperature, crystallization pressure and the amount of restricted crystals [31]. A poromechanical damage model based on crystallization pressure in a homogeneous state was proposed, and it showed that the expansion of cementitious materials increased with the amount of ettringite crystals and the crystallization pressure [32,33]. In the CSA cement paste, the crystal hydration product AFt or AFm can generate crystallization pressure, and the pressure exerted on the pore walls induces microstructural deformation of the matrix, resulting in expansion of the cement pastes [34]. So far, the physical and mechanical effect of crystal crystallization in pores have not yet been treated as an independent subject [35].

Cement paste is a complex porous material, primarily composed of the hydration products that can be categorized into crystal (calcium hydroxide (CH), ettringite, or monosulfoaluminate) [36–38] and gel (calcium silicate hydrate (C-S-H) or aluminum hydroxide gel (AH_3)) phases [39,40] based on their crystallinity. The gel products form a continuous matrix with pores and the crystals grow within these pores. It plays a critical role in volume change of cement paste [41]. According to the hypothesis "centroplasm hypothesis" for cementitious materials [42], the properties of cement paste are affected not only by the micro centroplasm (crystal phase) and micro medium (gel phase) but also by the interactions between the two phases [43,44]. Existing studies on volume change of cement paste mostly focus on the properties of the crystal products themselves, while ignoring the gel products and the interactions between crystal and gel products. In addition, the pore solution chemistry is not easy to obtain [33]. Therefore, the study on the properties of cementitious based on the crystallization pressure requires further improvement.

Solvent replacement techniques are commonly used to study and analyze the properties of cementitious materials, with ethanol and isopropyl alcohol being frequently employed solvents [45,46]. It has been observed that cement paste exhibited shrinkage during isopropyl alcohol replacement, which was attributed to three mechanisms: different diffusion speeds of water and IPA, osmotic extraction and chemical interaction [47]. A necessary condition for generating crystallization pressure is the occurrence of ion exchange between the crystal and the solution [48]. Calcium hydroxide and ettringite, the main crystal products of cement paste, are almost insoluble in isopropanol [49,50]. When the pore solution in cement paste is replaced by isopropyl alcohol, the crystallization pressure dissipates. Therefore, it should be one of the reasons for the shrinkage of cement paste.

In the present study, the volume change of cementitious materials affected by the interactions between crystal and gel products based on the crystallization pressure was discussed. A Theoretical model based on the interactions was developed to describe and calculate the volume change of cementitious materials. In the followed experiment, the crystallization pressure, which affects the interactions between crystal and gel products, was tailored by immersing specimens in different exchange solvents or solutions to change the solubility product in the pore solution. Water, isopropyl alcohol, ethanol, calcium hydroxide and calcium acetate with different concentrations were selected as the exchange solvents or solutions. The ion concentrations were tested by inductively-coupled plasma mass spectrometry and ion chromatography to calculate the crystallization pressure. In addition, the volume changes of cement pastes with different crystallization pressure in pore solution exchange and vacuum drying process were tested to discuss the effect of the interactions between crystal and gel hydration products on volume change of cementitious materials.

2. Theoretical analysis of the volume change based on the interactions between crystal and gel products

2.1 The interactions between crystal and gel products in cementitious materials

Cement paste expansion requires two key conditions: 1) the growth of hydration products should be restricted and 2) the expansive stress should be generated [51]. For Portland cement, the gel hydration products (C-S-H) exhibit limited expansion compared to the crystal hydration products (CH). Due to the limited capacity of CH to adsorb water molecules, the primary source of expansion might be the crystallization pressure generated by the restricted growth of CH.

Fig. 1 (a–e) illustrate the interactions between crystal and gel hydration products in cement paste, along with their formation and growth process. The crystals nucleate and grow within the pore spaces created by the gel phase (**Fig. 1(a)**), driven by the continued precipitation of ions from the supersaturated solution onto the growing crystal faces. When a crystal is restricted on both sides by the gel phase, its growth is restricted (**Fig. 1(b)**). However, according to the principles of crystallization kinetics, ions in a supersaturated pore solution can continue to be supplied to the restricted growth faces of a crystal through a thin liquid film (**Fig. 1(c)**). Restricted crystal growth within the gel phase can generate stress owing to the difference in the chemical potential between the crystal and the surrounding pore solution. This stress, known as crystallization pressure, is exerted on the gel, inducing internal stress (σ_{gel}) within the gel structure (**Fig. 1(d)**). It can cause the gel to undergo volumetric expansion (ε_{gel}) until an equilibrium is reached, where the stress exerted on the restricted crystal reaches the maximum crystallization pressure P_{cry}. Under drying conditions, the complete evaporation of the pore solution eliminates the liquid film between the gel and the crystal. When the liquid film is absent, mass can no longer be transported from the solution to the restricted crystal, leading to the disappearance of crystallization pressure [28]. Consequently, theoretical analysis indicates that the original stress and strain within the crystal and gel products are altered. For example, the reduction in compressive stress on the crystal products reduces their previous compressive deformation, while the reduction in tensile stress on gel products diminishes the prior tensile deformation. During this process, since the elastic modulus of the crystal products is higher than that of the gel products, the latter undergo more pronounced deformation. Consequently, the disappearance of the crystallization pressure results in the overall shrinkage (ε_{sh})

of the cement paste (**Fig. 1(e)**). In summary, theoretical analysis suggests that the interactions between crystal and gel products may alter the internal stress state of the hydration products, ultimately leading to changes in volume and mechanical properties of the cement paste. This paper aims to study the effect of the interactions between crystal and gel hydration products on the volume change of cementitious materials.

Fig. 1. The interactions between crystal and gel products in cement paste.

2.2 Theoretical model for the volume change of cement paste

Our previous study [52], combined with the analysis of interactions between crystal and gel hydration products, suggested that the volume change of cement paste during hydration can be categorized into four distinct stages. **Fig. 2** illustrates the interactions, the volume change and microstructural development of the cementitious materials at different stages.

Fig. 2. Simplified model of volume change and microstructural development of cementitious materials.

Stage I represents the early hydration period, which occurs before the cement paste hardens. During this stage, the gel phase (shown in gray) grows on the surface of the unhydrated cement particles (black), while crystals (blue) begin to form within the pore spaces. Moreover, the gel phase has not yet formed a continuous network, and the interactions between crystal and gel products are limited. Therefore, the cement paste exhibits a relatively small volume change.

As the gel phase develops into a continuous network throughout the cement paste, typically after hardening, **Stage II** commences. Earlier in **Stage II**, the gel phase forms a continuous network with interconnected pores. However, crystals within these pores typically do not yet contact the pore walls at either end, which means that the growth of crystals is still not restricted. Therefore, the interactions between crystal and gel products do not occur in the early period of **Stage II**, resulting in a minimal volume change of the cement paste.

Later in **Stage II**, as the hydration proceeds, the crystals within the pores continue to grow and contact with the surrounding gel network, and interactions between crystal and gel products occur. The pore solution ions remain in a supersaturated state throughout the hydration process. Based on the principles of crystallization kinetics, the ongoing growth of stressed crystals (red) within the pores generates crystallization pressure. This pressure exerts a tensile stress (σ_{gel}) on the surrounding gel phase and a compressive stress (σ_{cry}) on the crystal phase. As the volume of the stressed crystals increases further, the interactions between the gel and crystal products increase, leading to increased expansion of the cement paste.

Stage III commences when the hydration degree is high, and the amount of hydration products and the concentration of ions in the pore solution reach a relatively constant state. During this stage, the interactions between crystal and gel hydration products tend to remain relatively stable, resulting in a relatively stable volume of the cement paste.

However, a mismatched generation of the gel and crystal products or the excessive crystallization pressure leads to an imbalance in the interaction between crystal and gel products, causing the gel to experience excessive tensile stress, which commences **Stage IV**. Once the tensile stress of the gel phase exceeds its tensile strength, microcracks are formed within the gel network. This reduces the ability of cracked gel phases to restrict the growth of crystals, potentially leading to the further extension of microcracks. Complete penetration of microcracks through a section diminishes the gel phase's ability to constrain crystal growth, resulting in excessive expansion and eventual cement paste failure.

2.3 Mathematical model for the volume change of cement paste in water-saturated condition

In cement paste, gel hydration products constitute a porous continuous phase (such as C-S-H or AH_3) and crystal hydration products (such as CH, AFt, or AFm) develop within these pores. Drawing upon the principles of poroelasticity [32], a relationship between the expansion of cement pastes and the interactions between crystal and gel products was established as follows:

Consider a cement paste sample with volume V, comprising a gel phase (V_g), a crystal phase (V_c), and an interconnected pore space (V_p), such that the total volume V is the sum of these three volumes:

$$V = V_g + V_c + V_p \tag{1}$$

The porosity (ϕ) is defined as follows:

$$\phi = \frac{V_p}{V} = \frac{V_p}{V_g + V_c + V_p} \tag{2}$$

Under unconstrained conditions, the volume change of the cement paste is influenced by the interactions between crystal and gel products, which are driven by the crystallization pressure (P_{cry}) defined in **Eq. 3** [27]. The volumetric strains are selected as kinematic variables to formulate the constitutive equations for volumetric deformation.

$$P_{cry} = \frac{R_g \cdot T}{V_{cry}} \ln\left(\frac{Q^{ion}}{K^{ion}}\right) \tag{3}$$

where, R_g is the gas constant; T is the absolute temperature; V_{cry} is the molar volume of the crystal; K^{ion} is the equilibrium solubility; and Q^{ion} is the solubility product.

$$\frac{\Delta V}{V} = -\frac{1}{K}\left(-\alpha \cdot \kappa_{eff} P_{cry}\right) \tag{4}$$

$$\frac{\Delta V_{\mathrm{p}}}{V_{\mathrm{p}}} = -\frac{1}{K_{\mathrm{p}}}\left(-\beta \cdot \kappa_{\mathrm{eff}} P_{\mathrm{cry}}\right) \tag{5}$$

$$\frac{\Delta V_{\mathrm{c}}}{V_{\mathrm{c}}} = -\frac{1}{K_{\mathrm{c}}}\left(-\gamma \cdot \kappa_{\mathrm{eff}} P_{\mathrm{cry}}\right) \tag{6}$$

where, κ_{eff} denotes the volume coefficient of stressed crystals; K, K_{p}, and K_{c} denote the bulk moduli of cement paste, pore volume and crystal, respectively; α, β, and γ are the effective stress coefficient of cement paste, pore volume and crystal, respectively.

According to our previous study, the volume coefficient of stressed crystals κ_{eff} can be expressed as [53]:

$$\kappa_{\mathrm{eff}} = 1 - \mathrm{e}^{-\frac{0.3}{\phi}} \tag{7}$$

The effective stress coefficients and bulk moduli are related as follows [54]:

$$\alpha = 1 - \frac{K}{K_{\mathrm{s}}'} \tag{8}$$

$$\beta = 1 - \frac{K_{\mathrm{p}}}{K_{\mathrm{s}}''} \tag{9}$$

$$\gamma = 1 - \frac{K_{\mathrm{c}}}{K_{\mathrm{s}}'''} \tag{10}$$

where, K_{s}', K_{s}'', and K_{s}''' denote the bulk moduli of the skeleton (gel), pores, and crystals, respectively, in the unjacketed test.

The porosity variation $\Delta\phi$ can be obtained as follows:

$$\Delta\phi = \Delta\left(\frac{V_{\mathrm{p}}}{V}\right) = \frac{\Delta V_{\mathrm{p}} - \phi \Delta V}{V} \tag{11}$$

Based on **Eq. 1**, the following set of kinematic relations can be derived:

$$\frac{\Delta V}{V} = \frac{\Delta V_{\mathrm{g}} + \Delta V_{\mathrm{c}}}{V_{\mathrm{g}} + V_{\mathrm{c}}} + \frac{\Delta\phi}{1-\phi} \tag{12}$$

$$\frac{\Delta V_{\mathrm{p}}}{V_{\mathrm{p}}} = \frac{\Delta V_{\mathrm{g}} + \Delta V_{\mathrm{c}}}{V_{\mathrm{g}} + V_{\mathrm{c}}} + \frac{\Delta\phi}{(1-\phi)\phi} \tag{13}$$

Using the above equations, the volume variation of gel phase can be obtained as follows:

$$\frac{\Delta V_{\mathrm{g}}}{V_{\mathrm{g}}}=\frac{\Delta V}{V}\cdot\frac{1+R_{\mathrm{c/g}}}{1-\phi}-\frac{\Delta V_{\mathrm{p}}}{V_{\mathrm{p}}}\cdot\frac{\phi\left(1+R_{\mathrm{c/g}}\right)}{1-\phi}-\frac{\Delta V_{\mathrm{c}}}{V_{\mathrm{c}}}R_{\mathrm{c/g}} \tag{14}$$

where, $R_{\mathrm{c/g}}$ denotes the volume ratio of the crystals to the gel phase ($R_{\mathrm{c/g}} = V_{\mathrm{c}}/V_{\mathrm{g}}$).

Assuming the cement paste to be an ideal porous medium, the solid and pore spaces are deformed in the same proportion, which can be expressed as follows:

$$\frac{\Delta V}{V}=\frac{\Delta V_{\mathrm{g}}}{V_{\mathrm{g}}}=\frac{\Delta V_{\mathrm{p}}}{V_{\mathrm{p}}}=\frac{\Delta V_{\mathrm{c}}}{V_{\mathrm{c}}} \tag{15}$$

The crystal morphology affects the interactions between the hydration products, which in turn affects the volume change of the cement paste. The shape factor κ_{shape} is introduced to characterize the influence of crystals with different morphologies on the volume change of cement paste. In this study, the κ_{shape} values for AFt, CH and AFm were set to 1, 2/3 and 2/3, respectively.

Substituting **Eqs. 4–6** into **Eq. 14**, the stress-strain equation for the gel phase based on the crystallization pressure can be obtained as follows:

$$\varepsilon_{\mathrm{exp}}=\frac{\left(\kappa_{\mathrm{eff}}\kappa_{\mathrm{shape}}P_{\mathrm{cry}}\right)}{K_{\mathrm{s}}}\left[\frac{\alpha}{(1-\alpha)}\cdot\frac{1+R_{\mathrm{c/s}}}{1-\phi}-\frac{\beta}{(1-\beta)}\cdot\frac{\phi\left(1+R_{\mathrm{c/s}}\right)}{1-\phi}-\frac{\gamma}{(1-\gamma)}R_{\mathrm{c/s}}\right] \tag{16}$$

Thus, the change in cement paste volume due to the interactions between crystal and gel products can be computed using **Eq. 16**. The strain on cement paste is affected by crystallization pressure (P_{cry}), volume ratio of crystal to gel phase ($R_{\mathrm{c/g}}$) and the porosity (ϕ).

2.4 Mathematical model for the volume change of cement paste in drying condition

The interactions between crystal and gel products in the cement hydration products arise from the crystallization pressure. Crystallization pressure generated when the growth of crystals in a supersaturated solution is constrained and a liquid film exists between the crystal and the gel phases. However, the liquid film is disrupted during drying, eliminating the crystallization pressure, resulting in shrinkage of the cement paste. Therefore, the stress unloading of the interactions between crystal and gel products in the cement hydration products should be considered as one of the origins of drying shrinkage.

Existing studies primarily attribute the total shrinkage strain in cement paste to three mechanisms: capillary forces, solid surface tension, and disjoining pressure. The RH ranges required for operation of these three mechanisms are listed in **Table 1**. The drying shrinkage of the three mechanisms can be mathematically expressed as shown below.

Capillary forces [10,55,56]:

$$\varepsilon_{\mathrm{cf}} = \left(\frac{1}{K} - \frac{1}{K_b}\right)\frac{S_w RT}{3M\nu_w}\int_{RH_1}^{RH_2} \mathrm{d}\ln(RH) \tag{17}$$

where, $\varepsilon_{\mathrm{cf}}$ denotes the drying shrinkage strain caused by capillary forces; K and K_b are the bulk moduli of cement paste and solid phase, respectively; S_w is the degree of water saturation; R and T denote the gas constant and temperature, respectively; M and v_w denote the molar mass and specific volume of water, respectively.

Solid surface tension [6,57]:

$$\varepsilon_{\mathrm{st}} = \frac{\rho_{\mathrm{cem}} S_s}{E}\cdot\frac{RT}{\bar{V}}\int_{RH_1}^{RH_2}\frac{V_l}{S_s}\mathrm{d}\ln(RH) \tag{18}$$

where, $\varepsilon_{\mathrm{st}}$ denotes the drying shrinkage strain caused by solid surface tension; ρ_{cem} is the density of cement paste; S_s is the specific surface area; E is the elastic modulus of the cement paste; $\bar{V}$ is the molar volume of adsorbed liquid; V_l is the volume of adsorbed liquid.

Disjoining pressure [14]:

$$\varepsilon_{\mathrm{dp}} = k\cdot\frac{3(1-2\nu_{\mathrm{cem}})}{E}\frac{RT}{MV_w}\int_{RH_1}^{RH_2}\frac{w_d}{\phi_s}\mathrm{d}\ln(RH) \tag{19}$$

where, $\varepsilon_{\mathrm{dp}}$ denotes the drying shrinkage strain caused by disjoining pressure; k is a proportional constant; ν_{cem} denotes the Poisson's ratio of cement paste; V_{w} denotes the molar volume of water; w_d is the water content in the small pores; and ϕ_{s} denotes the solid volume fraction.

Table 1 RH ranges for the three mechanisms responsible for volume change of cement paste.

However, the cement paste is initially in an expanded state due to the "pre-stress" applied by the interactions between crystal and gel products before drying. The "pre-stress" is then unloaded after drying. Therefore, the total drying shrinkage strain (ε_{ds}) of cement paste can be mathematically expressed as [14]:

$$\varepsilon_{ds} = \varepsilon_{c/g} + \varepsilon_{cp} + \varepsilon_{st} + \varepsilon_{dp} \tag{20}$$

where, $\varepsilon_{c/g}$ is the drying shrinkage strain caused by the unloading of the interactions between crystal and gel products, and $\varepsilon_{c/g} = \varepsilon_{exp}$.

To investigate the impact of the interactions between crystal and gel products on the volume change of the cement paste, multiple experiments were conducted by varying the crystallization pressure.

3. Experimental program

As expressed in **Eq. 16**, the volume change of cement paste, which is determined by the interactions between crystal and gel products, is affected by crystallization pressure (P_{cry}), volume ratio of crystal to gel phase ($R_{c/g}$) and the porosity (ϕ). The interactions between crystal and gel products arise from crystallization pressure. In the experiment, the effect of the interactions between crystal and gel hydration products on the volume change of cement paste was investigated by varying the crystallization pressure. To minimize the impact of the changes in the volume ratio of crystal to gel products and the porosity of cement paste, specimens with a high hydration degree and solutions or solvents that do not react with the hydration products were utilized. To vary the crystallization pressure, solvent or solution exchange experiments were conducted to change the pore solution in the cement paste. The volume change of cement pastes with different crystallization pressures was tested during the solvent/solution exchange and vacuum drying processes to explore the influence of the interactions between crystal and gel products on the volume change of cement paste.

3.1 Raw materials

The cement used was P·O 42.5 and its chemical and phase composition is shown in **Table 2.** Ethanol and isopropyl alcohol were used as exchange solvents in this study. Calcium hydroxide, sodium hydroxide, and calcium acetate powders were used to prepare exchange solutions. The properties of the solvents and solutions are listed in **Table 3**.

Table 2 Chemical composition of the Portland cement.

Table 3 Properties of solvents and solutions.

3.2 Sample preparation

Cement pastes with water-to-binder (w/b) ratios of 0.5, were prepared according to the Chinese standard JC/T 313–2009. The specimens were cast and placed in steel molds of 25×25×280 mm^3, demolded after 24 h, and stored in water at 40°C to accelerate hydration for 28 days. A total of 36 identical specimens were prepared and divided into six groups.

3.3 Test methods

3.3.1 Overview of the whole process

The entire process was divided into two parts: solvent/solution exchange followed by vacuum drying, as shown in **Fig. 3**. X-ray diffraction (XRD) analysis, thermogravimetric analysis (TGA), ion and element concentration tests, mercury intrusion porosimetry (MIP) and nitrogen adsorption were used to study the properties of the cement pastes.

Fig. 3. Solvent/solution exchange and vacuum drying processes.

3.3.2 Solvent or solution exchange process

The length and mass of the cured specimens were measured and defined as the initial length L_0 and initial mass m_0. The specimens were placed in a water tank filled with exchange solvents or solutions and sealed. The length and mass of each specimen were measured every seven days, and the solvents or solutions were renewed. The solvent or solution exchange process was considered complete when the rate of change in length and mass between the last measurement and the previous one did not exceed ±0.02%. Inductively-coupled plasma mass spectrometry (ICP–MS) and ion chromatography (IC) were used to analyze the concentrations of ions and elements in the replacing solvents and solutions at the conclusion of the exchange process. The length change rates of the specimens were calculated using **Eq. 21** according to the Chinese standard JC/T 313–2009.

$$\Delta L = \frac{L_t - L_0}{250} \times 100\% \tag{21}$$

where, ΔL denotes the rate of change in the length of the specimen after solvent or solution exchange (%); L_0 is the initial length of the specimen; L_t is the length of the specimen after solvent or solution exchange.

3.3.3 Vacuum drying process

After solvent or solution exchange process, specimens were placed into a vacuum dryer controlled at approximately 40°C. The length and mass of each specimen were measured every seven days. The vacuum drying process was completed when the rate of change in length and mass between the last measurement and the previous one did not exceed ±0.02%. Subsequently, parts of the specimens from each group were used to prepare samples for TGA, XRD, MIP, and nitrogen adsorption analyses.

3.3.4 Ion concentration analysis

To determine the crystallization pressure, the anion concentration in the soaking solution after solution exchange was determined by ion chromatography (IC). The deionized water used in the laboratory had a conductivity of 18.2 MΩ/cm, and a 0.2 μm disposable microporous filter membrane was used. The concentrations of the elements in the soaking solution were determined by inductively-coupled plasma mass spectrometry (ICP–MS).

3.3.5 Thermogravimetric analysis

To characterize the types and contents of hydration products, thermogravimetric analysis (TGA) testing was conducted. After vacuum drying process, the central fragments of the broken specimens were selected and ground into a fine powder in an agate mortar. The powder was then sieved through a 0.056 mm square sieve, and the sieved part was used for TGA testing. Then, the vacuum-dried samples were gradually heated at a rate of 10 °C /min till their temperature reached 900°C under a controlled N_2 atmosphere.

3.3.6 X–ray diffraction analysis

To characterize the types and contents of crystal products, X–ray diffraction (XRD) testing was conducted. The sample preparation for this experiment followed the same procedure as for the TGA test. Before the test, 10% α–Al_2O_3 was used as an internal standard. The measurement range was 5–70° with a step size of 0.02°.

3.3.7 Mercury intrusion porosimetry analysis

To characterize the porosity of the cement paste, Mercury intrusion porosimetry (MIP) testing was conducted. It was performed on the vacuum-dried cement paste samples. The samples were crushed into fragments of 5–7 mm diameter. The minimum and maximum pressures of the mercury porosimeter used for this experiment were 0.0014 and 420 MPa, respectively. The pore volume was obtained by controlling the applied external force and the amount of mercury intrusion.

3.3.8 Nitrogen adsorption tests

Nitrogen adsorption tests were performed on cement paste samples after vacuum drying to characterize the pore structure. The samples were crushed into pieces with diameters smaller than 5 mm. The samples were degassed under vacuum at liquid nitrogen temperature. Then, they were subjected to nitrogen adsorption and desorption at full humidity. The equilibrium points for the adsorption and desorption were set over the entire humidity range. The initial vacuum pressure was considered reached when the reading was less than 0.520 KPa.

4. Results and discussion

4.1 Ion concentration analysis in the final solvent or solution

For the Portland cement, the main crystal hydration products are calcium hydroxide (CH), ettringite (AFt) and AFm, which contain calcium (Ca^{2+}), hydroxide (OH^-), aluminate (AlO_2^-) and sulfate (SO_4^{2-}) ions. the concentrations of these key ions (Ca^{2+}, AlO_2^-, SO_4^{2-} and OH^-) were obtained using ICP–MS and IC analyses of the final solvent or solution and are shown in **Fig. 4 (a–d)**.

Fig. 4. Concentrations of Ca^{2+}, AlO_2^-, SO_4^{2-} and OH^- in different solvents and solutions (H_2O-water, IPA-isopropyl alcohol, ETH-ethanol, CH-calcium hydroxide, $CaAc_2$-calcium acetate, L-low concentration, H-high concentration).

4.2 Hydration products and porosity in cement pastes

The TGA curves of the specimens are shown in **Fig. 5**. It showed that the solution exchange and vacuum drying processes do not cause significant changes in the composition or mass fraction of the hydration products.

Fig. 5. TGA curves obtained for cement pastes immersed in different pore solvents or solutions (H_2O-water, IPA-isopropyl alcohol, ETH-ethanol, CH-calcium hydroxide, $CaAc_2$-calcium acetate, L-low concentration, H-high concentration).

The XRD patterns of the specimens are shown in **Fig. 6**. The results showed that the hydration products in the cement paste were not significantly affected by solution exchange and subsequent vacuum drying, which agrees with the observations from the TGA analysis. Therefore, the types and mass fractions of the hydration products identified in the water-immersed specimens were used to characterize the hydration products in all specimens. The types and contents of the main hydration products in the cement pastes are listed in **Table 4**.

Fig. 6. XRD patterns obtained for cement pastes immersed in different pore solvents or solutions (H_2O-water, IPA-isopropyl alcohol, ETH-ethanol, CH-calcium hydroxide, $CaAc_2$-calcium acetate, L-low concentration, H-high concentration).

Table 4 Types and contents of hydration products in cement paste.

The cumulative porosity curves of the specimens tested by MIP are shown in **Fig. 7**. The results showed that the porosities of the cement pastes after solution or solvent exchange remained mostly unchanged, which is consistent with findings of previous studies [58]. Therefore, the porosity of 34.28% measured in the water-immersed specimen was considered representative of the porosity of all specimens.

Fig. 7. Pore size distribution of cement pastes immersed in different pore solvents or solutions obtained from MIP tests (H_2O-water, IPA-isopropyl alcohol, ETH-ethanol, CH-calcium hydroxide, $CaAc_2$-calcium acetate, L-low concentration, H-high concentration).

4.3 Deformation of cement pastes throughout the solvent/solution exchange and vacuum drying processes

Fig. 8(a-c) illustrates the length change rates of the cement pastes throughout the solvent/solution exchange and vacuum drying processes. Compared with the reference group (specimens immersed in water), specimens immersed in calcium hydroxide (CH) and calcium acetate ($CaAc_2$) solutions exhibited expansion during the exchange process, whereas those immersed in isopropyl alcohol (IPA) and ethanol (ETH) solvents experienced shrinkage. All specimens shrank during the vacuum drying process. In particular, the specimens immersed in solvents showed lower shrinkage than the other specimens.

Fig. 8. (a) Length change of specimens throughout the whole process, (b) length change of specimens during solvent/solution exchange process and (c) length change of specimens during

vacuum drying process (H_2O-water, IPA-isopropyl alcohol, ETH-ethanol, CH-calcium hydroxide, $CaAc_2$-calcium acetate, L-low concentration, H-high concentration).

4.3.1 Deformation of cement pastes during solvent or solution exchange process

Fig. 8(b) illustrates the length change rates of the cement pastes during the solvent or solution exchange processes. The specimens immersed in high-concentration calcium acetate solutions ($CaAc_2$-H) expanded the most, whereas those immersed in other solutions exhibited similar expansions. On the other hand, specimens in which the pore solution was replaced with isopropyl alcohol (IPA) and ethanol (ETH) exhibited shrinkage.

The analysis of the interactions between crystal and gel hydration products in **Section 2.3** may explain the expansion of the cement paste. A direct study of the interactions between crystal and gel products in cement pastes is challenging. However, the crystallization pressure can be represented by experimental results and serves as an indirect indicator of the interactions. The interactions between crystal and gel products originate from the crystallization pressure, which is directly affected by the solubility product in the pore solution. A higher solubility product leads to a greater crystallization pressure, signifying stronger the interactions between crystals and gel hydration products. In solvent or solution exchange experiments, the pore solutions were replaced with different solvents and solutions. The hydration products AFt, AFm, and CH can generate crystallization pressure, the average crystallization pressure defined in **Eq. 22** was used to characterize the pressure within the cement paste.

$$P_{\mathrm{cry}}^{\mathrm{ave}}=\frac{\kappa_{\mathrm{shape,CH}}\cdot P_{\mathrm{cry}}^{\mathrm{CH}}V_{\mathrm{CH}}+\kappa_{\mathrm{shape,AFt}}\cdot P_{\mathrm{cry}}^{\mathrm{AFt}}V_{\mathrm{AFt}}+\kappa_{\mathrm{shape,AFm}}P_{\mathrm{cry}}^{\mathrm{AFm}}V_{\mathrm{AFm}}}{V_{\mathrm{CH}}+V_{\mathrm{AFt}}+V_{\mathrm{AFm}}} \quad (22)$$

where, $P_{\mathrm{cry}}^{\mathrm{ave}}$ denotes the average crystallization pressure of all crystals; V_{x} denotes the volume of crystal phase x; $P_{\mathrm{cry}}^{\mathrm{x}}$ denotes the crystallization pressure generated by phase x.

Combined with the results in **Fig. 4** and **Table 4**, the average crystallization pressure for different cement pastes were calculated and is provided in **Table 5**. Building on the calculated crystallization pressures in different solvents and solutions, the results of solvent or solution exchange experiments (**Fig. 8(b)**) indicate that the specimen dimensions change in response to variations in the crystallization pressure.

Table 5 Average crystallization pressure for different cement pastes.

The observed volume change of the cement paste during the solvent or solution exchange process may arise from factors other than the interactions between crystal and gel hydration products, such as changes in the hydration products, porosity, and solid surface energy. The results of TGA, XRD, and MIP experiments and literature findings [47,59–61] indicate that the hydration products and porosity of Portland cement paste immersed in water (H_2O), calcium hydroxide (CH), ethanol (ETH), isopropyl alcohol (IPA), and calcium acetate ($CaAc_2$) remain mostly unchanged. Replacing the pore solution of the cement paste with organic solvents may alter the surface energy of the solid phase, potentially leading to volume changes. Theoretical calculations based on surface energy changes suggested that replacing the pore solution with ETH or IPA should cause the cement paste to expand. However, the experimental results contradicted this prediction, as the specimens contracted after solvent exchange. This observation was consistent with previous findings reported in the literature [62]. Therefore, based on the theoretical analysis in this study, the volume change of the cement paste after solvent or solution exchange was considered to be caused by a change in the interactions between crystal and gel hydration products.

The expansion of the cement pastes after solution exchange was calculated using **Eq. 16** by incorporating the experimental results. The bulk moduli of C-S-H [63], CH [64], AFt [65] and AFm [66] are 14–19 GPa, 20–25 GPa, 24–30 GPa, and 40 GPa, respectively. The calculated expansion of cement pastes with different crystallization pressures were compared with the actual volume changes observed experimentally, as shown in **Fig. 9**. It can be seen from **Fig. 8(b)** that the shrinkage of the specimens immersed in ethanol was less than that of the specimens immersed in isopropyl alcohol during the solvent/solution exchange process. It may be related to the reaction or absorption between ethanol and hydration products [47]. In the followed analysis, the final length of the IPA specimen in pore solution exchange process was set as the baseline (zero) because it has no crystallization pressure and negligible volume changes caused by interactions between crystal and gel hydration products. Both the experimental and calculated results demonstrated a positive correlation between the expansion and crystallization pressures. The calculated and measured values were in good agreement with each other. **Table 5** and **Fig. 9** showed that a 45.3% increase in crystallization pressure resulted in a 46.1% increase in expansion. Higher crystallization pressure enhanced the interactions between crystal and gel products, ultimately leading to greater expansion. In addition, Eq. 16, which was established based on the interactions between crystal and gel products, indicates that the expansion of cement paste exhibits a positive linear relationship with crystallization pressure when the volume of hydration products and porosity are constant. The experimental observations aligned with the established equation. Therefore, the results support the role of the interactions between crystal and gel hydration products in influencing the expansion of cement paste. As the interactions intensified, the observed expansion increased.

Fig. 9. Expansion of cement pastes within different crystallization pressures (H_2O-water, CH-calcium hydroxide, $CaAc_2$-calcium acetate, L-low concentration, H-high concentration).

4.3.2 Deformation of cement pastes during vacuum drying process

The length change rates of the cement pastes during the vacuum drying process are shown in **Fig. 8(c)**. The end of the solvent or solution exchange process marks the zero point of shrinkage. The specimens immersed in water (H_2O), calcium hydroxide (CH), and low-concentration calcium acetate ($CaAc_2$-L) exhibited similar extents of drying shrinkage. This shrinkage is substantially greater than that of specimens immersed in ethanol (ETH) and isopropyl alcohol (IPA), and marginally lower than the shrinkage observed in specimens immersed in a high concentration of calcium acetate ($CaAc_2$-H).

As analyzed in **Section 2.4**, the gel phase is under a "pre-stress" state that contributes to the expansion of cement paste when saturated with water due to the interactions between crystal and gel hydration products. Upon complete drying of the cement paste, both the crystallization pressure and the interactions between crystal and gel hydration products become negligible, causing the original expansion deformation to disappear. Therefore, the weakening or disappearance of the interactions between crystal and gel hydration products may be a factor that contributes to the drying shrinkage deformation of the cement paste.

As illustrated in **Fig. 8(c)**, the specimen immersed in a high concentration of calcium acetate ($CaAc_2$-H) exhibited the largest final drying shrinkage strain. Specimens immersed in water (H_2O), calcium hydroxide (CH), and low-concentration calcium acetate ($CaAc_2$-L) showed a similar level of shrinkage strain, which was lower than that of $CaAc_2$-H but higher than that of both ethanol (ETH) and isopropyl alcohol (IPA), which exhibited a minimal shrinkage strain. The results of this analysis suggest that the drying shrinkage strain in cement paste results from a combination of several factors including capillary forces, changes in surface tension, disjoining pressure, and the interactions between crystal and gel hydration products. However, according to the conclusion presented by Babaei [14], capillary forces do not operate in a low RH environment, such as the end of a vacuum drying process in this research. Therefore, the shrinkage caused by capillary forces was ignored in the subsequent calculation of the final drying shrinkage of cement paste. Compared to specimens immersed in H_2O, CH, and $CaAc_2$-L, that immersed in $CaAc_2$-H exhibits stronger the interactions between crystal and gel hydration products, which possibly contributes to its higher final drying shrinkage strain. In contrast, specimens immersed in ETH and IPA had a greater molar volume of adsorbed liquid and minimal interactions between crystal and gel products, resulting in a lower final drying shrinkage strain. The isothermal adsorption-desorption curve of the cement paste is shown in **Fig. 10**. It has been reported that surface tension is linearly proportional to the total surface area, as determined from volume-thickness (V-t) sorption analysis, with V-t curves constructed from the isothermal adsorption-desorption curve [6,57]. Therefore, in combination with **Eq. 18**, the drying shrinkage caused by surface tension can be calculated. Similarly, the water content in small pores (w_d), a key parameter in the disjoining pressure equation (**Eq. 19**), can also be obtained from the isothermal adsorption-desorption curve [14], allowing for the calculation of drying shrinkage caused by disjoining pressure.

Fig. 10. Isothermal adsorption-desorption curve of the cement paste.

Based on **Eq. 20**, the shrinkage caused by each individual mechanism and the total shrinkage strain can be calculated theoretically. The correlation between the calculated drying shrinkage and the experimentally measured values is illustrated in **Fig. 11**. The calculated and measured values are in good agreement with each other. Therefore, in addition to capillary forces, solid surface tension, and disjoining pressure, the disappearance of the interactions between crystal and gel hydration products is another factor contributing to the drying shrinkage of cement paste.

Fig. 11. Drying shrinkage of cement pastes (H_2O-water, CH-calcium hydroxide, $CaAc_2$-calcium acetate, L-low concentration, H-high concentration).

5. Conclusions

To study the effect of the interactions between crystal and gel products on the volume change of cementitious materials, the crystallization pressure of crystal products was tailored by changing the solubility product in the pore solution. In addition, theoretical model based on the interactions between crystal and gel products have been proposed and established to describe the volume change of cementitious materials. The following conclusions were drawn.

(1) The ion concentrations (or solubility product) in the pore solution of cement pastes are altered by immersing them in different solvents or solutions (such as water, isopropyl alcohol, ethanol, calcium hydroxide and calcium acetate with various concentrations), thereby changing the crystallization pressure of crystal products in the cement pastes and ultimately affecting the volume change of these cement pastes on the macro scale.

(2) The interactions between crystal and gel products affects the expansion of cementitious materials. Crystallization pressure, which affects the interactions directly, shows a positive correlation with the expansion of cement pastes. In cement pastes with similar hydration product formation and pore structures, a 45.3% increase in crystallization pressure resulted in a 46.1%

increase in expansion. Higher crystallization pressure leads to stronger interactions between crystal and gel products, causing greater tensile stress in the gel products and ultimately resulting in more significant expansion of the cementitious materials.

(3) The interactions between crystal and gel products affects the drying shrinkage of cementitious materials. Cement pastes with higher crystallization pressure exhibits greater shrinkage. Water removal (such as during the drying process) from cement paste can eliminate the crystallization pressure, thereby reducing the interactions between crystal and gel products. As a result, the original expansion caused by the interactions disappears, ultimately leading to the drying shrinkage of cement paste. In addition to the changes in capillary forces, solid surface tension, and disjoining pressure, the reduction in the interactions between crystal and gel products should be considered as one of the mechanisms for the drying shrinkage of cementitious materials.

(4) The established theoretical model analyzed the expansion and drying shrinkage of cementitious materials based on the interactions between crystal and gel products. The results calculated by the model are in good agreement with the experimental results.

6. Future work

The interactions between crystal and gel products should be considered one of the mechanisms for the volume change in cementitious materials. In future work, the proportion of volume change caused by the interactions relative to the total volume change will be studied. Other factors that affecting the interactions between crystal and gel products (such as the volume of crystal and gel products, porosity and temperature) also will be studied. In addition, some microscopic experiments will be meticulously designed to verify the interactions between crystal and gel products in cementitious materials.

Acknowledgment

The authors would thank Tangshan Polar Bear Building Materials Co., Ltd for providing the necessary equipment to perform the experimental work of this research.

Author contributions:

Depeng Zhang: Conceptualization, Methodology, Validation, Writing - Original Draft. **Hui Li**: Methodology, Writing - Review & Editing. **Zhenyu Pi**: Methodology, Writing - Review & Editing. **Mingfeng Xu**: Writing - Review & Editing, Funding acquisition. **Jian Zhou**: Conceptualization, Resources, Supervision, Funding acquisition. **Mingzhong Zhang**: Writing - Review & Editing.

Funding:

This work was supported by the Major Program of the National Natural Science Foundation of China [grant numbers 52293434]; National Natural Science Foundation of China [grant numbers 52178200]; the Natural Science Foundation of Hebei Province, China [Grant No. E2022202124]; and the China Scholarship Council.

References

[1] M.C.G. Juenger, H.M. Jennings, Examining the relationship between the microstructure of calcium silicate hydrate and drying shrinkage of cement pastes, Cem. Concr. Res. 32 (2002) 289–296. https://doi.org/10.1016/S0008-8846(01)00673-1.

[2] K. Shuldyakov, B. Trofimov, L. Kramar, Stable microstructure of hardened cement paste–A guarantee of the durability of concrete, Case Stud. Constr. Mater. 12 (2020) e00351. https://doi.org/10.1016/j.cscm.2020.e00351.

[3] A.M. Neville, J.J. Brooks, Concrete Technology, second ed., Longman Scientific & Technical, London, 1987.

[4] C.T. Nguyen, D.T. Ho, S.Y. Kim, An Enhanced Sampling Approach for Computing the Free Energy of Solid Surface and Solid–Liquid Interface, Adv. Theory Simul. 7 (2024) 2300538. https://doi.org/10.1002/adts.202300538.

[5] C. Di Bella, M. Wyrzykowski, P. Lura, Evaluation of the ultimate drying shrinkage of cement-based mortars with poroelastic models, Mater. Struct. 50 (2017) 1–13. https://doi.org/10.1617/s11527-016-0870-0.

[6] J.A. Almudaiheem, Prediction of drying shrinkage of Portland cement paste: influence of shrinkage mechanisms, J. King Saud Univ. Sci. 3 (1991) 69–86. https://doi.org/10.1016/S1018-3639(18)30538-5.

[7] M.B. Pinson, E. Masoero, P.A. Bonnaud, et al., Hysteresis from multiscale porosity: modeling water sorption and shrinkage in cement paste, Phys. Rev. Appl. 3 (2015) 64009. https://doi.org/10.1103/PhysRevApplied.3.064009.

[8] H. J. Butt, M. Kappl, Normal capillary forces, Adv. Colloid Interface Sci. 146 (2009) 48–60. https://doi.org/10.1016/j.cis.2008.10.002.

[9] P. Schiller, M. Wahab, T. Bier, et al., A model for sorption hysteresis in hardened cement paste, Cem. Concr. Res. 123 (2019) 105760. https://doi.org/10.1016/j.cemconres.2019.05.005.

[10] K. Kovler, S. Zhutovsky, Overview and future trends of shrinkage research, Mater. Struct. 39 (2006) 827–847. https://doi.org/10.1617/s11527-006-9114-z.

[11] F.H. Wittmann, Heresies on shrinkage and creep mechanisms, Proceedings of Creep, Shrinkage and Durability Mechanics of Concrete and Concrete Structures, London: Taylor and Francis Group, (2009) 3–10.

[12] B.V. Derjaguin, N.V. Churaev, V.M. Muller, et al., Surface forces, Springer, New York, 1987. https://doi.org/10.1007/978-1-4757-6639-4.

[13] T.C. Powers, The thermodynamics of volume change and creep, Mater. Struct. 1 (1968) 487–507. https://doi.org/10.1007/BF02473638.

[14] S. Babaei, S.C. Seetharam, A. Dizier, et al., An analytical framework for estimating drying shrinkage strain of OPC based hardened cement paste, Cem. Concr. Compos. 115 (2021) 103833. https://doi.org/10.1016/j.cemconcomp.2020.103833.

[15] H. Nguyen, S. Rahimi-Aghdam, Z.P. Bažant, Unsaturated nanoporomechanics, P. Natl. Acad. Sci. USA 117 (2020) 3440–3445. https://doi.org/10.1073/pnas.1919337117.

[16] M. Polivka, Factors influencing expansion of expansive cement concretes, in ACI SP-38, (1973) 239–250. https://doi.org/10.14359/17206.

[17] J. Bizzozero, Hydration and Dimensional Stability of Calcium Aluminate Cement Based Systems, Doctoral thesis EPF Lausanne, Lausanne, 2014. https://doi.org/10.5075/epfl-thesis-6336.

[18] D. Torréns-Martín, L. Fernández-Carrasco, Effect of sulfate content on cement mixtures, Constr. Build. Mater. 48 (2013) 144–150. https://doi.org/10.1016/j.conbuildmat.2013.05.106.

[19]T. Desbois, R. Le Roy, A. Pavoine, et al., Effect of gypsum content on sulfoaluminate mortars stability, Eur. J. Environ. Civ. Eng. 14 (2010) 579–597. https://doi.org/10.1080/19648189.2010.9693248.

[20]H.F.W. Taylor, C. Famy, K.L. Scrivener, Delayed ettringite formation, Cem. Concr. Res. 31 (2001) 683–693. https://doi.org/10.1016/S0008-8846(01)00466-5.

[21]S. Taber, The growth of crystals under external pressure, Am. J. Sci. 246 (1916) 532–556. https://doi.org/10.2475/ajs.s4-41.246.532.

[22]Q. Wang, W. Wilson, K. Scrivener, Unidirectional penetration approach for characterizing sulfate attack mechanisms on cement mortars and pastes, Cem. Concr. Res. 169 (2023) 107166. https://doi.org/10.1016/j.cemconres.2023.107166.

[23]C. Yu, W. Sun, K. Scrivener, Mechanism of expansion of mortars immersed in sodium sulfate solutions, Cem. Concr. Res. 43 (2013) 105–111. https://doi.org/10.1016/j.cemconres.2012.10.001.

[24]M. Wagner, M. Decker, W. Kunther, et al., Gypsum formation mechanisms and their contribution to crystallisation pressure in sulfate resistant hardened cement pastes during early external sulfate attack at low sulfate concentrations, Cem. Concr. Res. 168 (2023) 107138. https://doi.org/10.1016/j.cemconres.2023.107138.

[25]G.W. Scherer, Supersaturation in porous media, in: Poromechanics V: Proceedings of the Fifth Biot Conference on Poromechanics, 2013: pp. 2290–2296. https://doi.org/10.1061/9780784412992.268.

[26]J. Desarnaud, D. Bonn, N. Shahidzadeh, The pressure induced by salt crystallization in confinement, Sci Rep 6, 30856 (2016). https://doi.org/10.1038/srep30856.

[27]C.W. Correns, Growth and dissolution of crystals under linear pressure, Discuss. Faraday Soc. 5 (1949) 267–271. https://doi.org/10.1039/DF9490500267.

[28] L. Li, F. Kohler, J. Dziadkowiec, et al., Limits to crystallization pressure, Langmuir. 38 (2022) 11265–11273. https://doi.org/10.1021/acs.langmuir.2c01325.

[29] M. Santhanam, M.D. Cohen, J. Olek, Mechanism of sulfate attack: A fresh look: Part 1: Summary of experimental results, Cem. Concr. Res. 32 (2002) 915–921. https://doi.org/10.1016/S0008-8846(02)00724-X.

[30] M. Santhanam, M.D. Cohen, J. Olek, Mechanism of sulfate attack: a fresh look: Part 2. Proposed mechanisms, Cem. Concr. Res. 33 (2003) 341–346. https://doi.org/10.1016/S0008-8846(02)00958-4.

[31] R.J. Flatt, G.W. Scherer, Thermodynamics of crystallization stresses in DEF, Cem. Concr. Res. 38 (2008) 325–336. https://doi.org/10.1016/j.cemconres.2007.10.002.

[32] Y. Gu, P. Dangla, R.-P. Martin et al., Modeling the sulfate attack induced expansion of cementitious materials based on interface-controlled crystal growth mechanisms, Cem. Concr. Res. 152 (2022) 106676. https://doi.org/10.1016/j.cemconres.2021.106676.

[33] Q. Huang, Q. Wang, X. Zhu, Contradict mechanism of long-term magnesium and sodium sulfate attacks of nano silica-modified cement mortars–Experimental and thermodynamic modeling, Cem. Concr. Compos. 147 (2024) 105444. https://doi.org/10.1016/j.cemconcomp.2024.105444.

[34] C.W. Hargis, B. Lothenbach, C.J. Müller, et al., Further insights into calcium sulfoaluminate cement expansion, Adv. Cem. Res. 31 (2019) 160–177. https://doi.org/10.1680/jadcr.18.00124.

[35] B. Ran, O. Omikrine-Metalssi, T. Fen-Chong, et al., Pore crystallization and expansion of cement pastes in sulfate solutions with and without chlorides, Cem. Concr. Res. 166 (2023) 107099. https://doi.org/10.1016/j.cemconres.2023.107099.

[36] I.G. Richardson, The nature of the hydration products in hardened cement pastes, Cem. Concr. Compos. 22 (2000) 97–113. https://doi.org/10.1016/S0958-9465(99)00036-0.

[37]J. Han, K. Wang, J. Shi, et al., Influence of sodium aluminate on cement hydration and concrete properties, Constr. Build. Mater. 64 (2014) 342–349. https://doi.org/10.1016/j.conbuildmat.2014.04.089.

[38]L.G. Baquerizo, T. Matschei, K.L. Scrivener, et al., Hydration states of AFm cement phases, Cem. Concr. Res. 73 (2015) 143–157. https://doi.org/10.1016/j.cemconres.2015.02.011.

[39]D. Hou, H. Ma, Z. Li, Morphology of calcium silicate hydrate (CSH) gel: a molecular dynamic study, Adv. Cem. Res. 27 (2015) 135–146. https://doi.org/10.1680/adcr.13.00079.

[40]Y. Zhang, J. Chang, J. Ji, AH_3 phase in the hydration product system of AFt-AFm-AH_3 in calcium sulfoaluminate cements: A microstructural study, Constr. Build. Mater. 167 (2018) 587–596. https://doi.org/10.1016/j.conbuildmat.2018.02.052.

[41]M.C.G. Juenger, H.M. Jennings, Examining the relationship between the microstructure of calcium silicate hydrate and drying shrinkage of cement pastes, Cem. Concr. Res. 32 (2002) 289–296. https://doi.org/10.1016/S0008-8846(01)00673-1.

[42]H Lian, H Shi, Clarification of a Hypothesis on ‘Centroplasm of Cement-based Composite’ Proposed by Wu Zhongwei, J. Chin. Ceram. Soc. 48 (2020) 777–786. https://doi.org/10.14062/j.issn.0454-5648.20200024. (in Chinese)

[43]D. Fan, J.-X. Lu, K. Liu, et al., Multi-scale design of ultra-high performance concrete (UHPC) composites with centroplasm theory, Compos. Part B-Eng. 281 (2024) 111562. https://doi.org/10.1016/j.compositesb.2024.111562.

[44]T. Yin, L. Jin, K. Liu, et al., Fractal evolution model of proton spatial distribution in low water/binder cement-based composites (LW/B-CC) during early-age hydration process, Constr. Build. Mater. 427 (2024) 136287. https://doi.org/10.1016/j.conbuildmat.2024.136287.

[45] J.J. Beaudoin, B. Tamtsia, J. Marchand, et al., Solvent exchange in partially saturated and saturated microporous systems: length change anomalies, Cem. Concr. Res. 30 (2000) 359–370. https://doi.org/10.1016/S0008-8846(99)00260-4.

[46] C. Zhou, F. Ren, Q. Zeng, et al., Pore-size resolved water vapor adsorption kinetics of white cement mortars as viewed from proton NMR relaxation, Cem. Concr. Res. 105 (2018) 31–43. https://doi.org/10.1016/j.cemconres.2017.12.002.

[47] Z. Zhang, G.W. Scherer, Supercritical drying of cementitious materials, Cem. Concr. Res. 99 (2017) 137–154. https://doi.org/10.1016/j.cemconres.2017.05.005.

[48] M. Steiger, Crystal growth in porous materials—I: The crystallization pressure of large crystals, J. Cryst. Growth 282 (2005) 455–469. https://doi.org/10.1016/j.jcrysgro.2005.05.007.

[49] J.J. Beaudoin, P. Gu, J. Marchand, et al., Solvent replacement studies of hydrated Portland cement systems: the role of calcium hydroxide, Adv. Cem. Based Mater. https://doi.org/10.1016/S1065-7355(98)00008-X.

[50] R. Khoshnazar, J. Beaudoin, L. Raki, et al., Solvent exchange in sulphoaluminate phases. Part I: ettringite, Adv. Cem. Res. 25 (2013) 314–321. https://doi.org/10.1680/adcr.12.00042.

[51]G.W. Scherer, Stress from crystallization of salt, Cem. Concr. Res. 34 (2004) 1613–1624. https://doi.org/10.1016/j.cemconres.2003.12.034.

[52]J Zhou, Z Chen, M Lan, et al., Effect of Ettringite on Volume Change and Mechanical Properties of Cementitious Materials, in: Workshop on Concrete Modelling and Materials Behavior in Honor of Professor Klaas van Breugel, Delft, 2018.

[53] D Zhang, H Li, Z Pi, et al., Volume change of cementitious materials affected by the interactions between crystal and gel products, J. Build. Mater. under review, submitted in 2024-08-08 (In Chinese).

[54]J.R. Rice, M.P. Cleary, Some basic stress diffusion solutions for fluid‐saturated elastic porous media with compressible constituents, Rev. Geophys. 14 (1976) 227‐241. https://doi.org/10.1029/RG014i002p00227.

[55]E.J. Garboczi, D.P. Bentz, Analytical formulas for interfacial transition zone properties, Adv. Cem. Based Mater. 6 (1997) 99–108. https://doi.org/10.1016/S1065-7355(97)90016-X.

[56]J. Mackenzie, The elastic constants of a solid containing spherical holes, Proc. Phys. Soc. B. 63 (1950) 2. https://doi.org/10.1088/0370-1301/63/1/302.

[57]W. Hansen, Drying shrinkage mechanisms in Portland cement paste, J. Am. Ceram. Soc. 70 (1987) 323–328. https://doi.org/10.1111/j.1151-2916.1987.tb05002.x.

[58]C. Zhou, F. Ren, Z. Wang, et al., Why permeability to water is anomalously lower than that to many other fluids for cement-based material, Cem. Concr. Res. 100 (2017) 373–384. https://doi.org/10.1016/j.cemconres.2017.08.002.

[59]X. Wang, A.B. Eberhardt, E. Gallucci, et al., Assessment of early age properties of cementitious system through isopropanol-water replacement in the mixing water, Cem. Concr. Res. 84 (2016) 76–84. https://doi.org/10.1016/j.cemconres.2016.02.009.

[60] J. Zhang, G.W. Scherer, Comparison of methods for arresting hydration of cement, Cem. Concr. Res. 41 (2011) 1024–1036. https://doi.org/10.1016/j.cemconres.2011.06.003.

[61]K. Cao, L. Wang, Y. Xu, et al., The hydration and compressive strength of cement mortar prepared by calcium acetate solution, Adv. Civ. Eng. 2021 (2021) 1–9. https://doi.org/10.1155/2021/8817725.

[62]Z. Zhang, G.W. Scherer, Physical and chemical effects of isopropanol exchange in cement-based materials, Cem. Concr. Res. 145 (2021) 106461. https://doi.org/10.1016/j.cemconres.2021.106461.

[63]G. Constantinides, F.J. Ulm, The effect of two types of CSH on the elasticity of cement-based materials: Results from nanoindentation and micromechanical modeling, Cem. Concr. Res. 34 (2004) 67–80. https://doi.org/10.1016/S0008-8846(03)00230-8.

[64]FH Wittmann, Estimation of the modulus of elasticity of calcium hydroxide, Cem. Concr. Res. 16 (1986) 971–972. https://doi.org/10.1016/0008-8846(86)90021-9.

[65]S. Speziale, F. Jiang, Z. Mao, et al., Single-crystal elastic constants of natural ettringite, Cem. Concr. Res. 38 (2008) 885–889. https://doi.org/10.1016/j.cemconres.2008.02.004.

[66]P. Termkhajornkit, Q.H. Vu, R. Barbarulo, et al., Dependence of compressive strength on phase assemblage in cement pastes: Beyond gel-space ratio-Experimental evidence and micromechanical modeling, Cem. Concr. Res. 56 (2014) 1–11. https://doi.org/10.1016/j.cemconres.2013.10.007.

Figure

Click here to access/download;Figure;Revised_Figures_print.docx

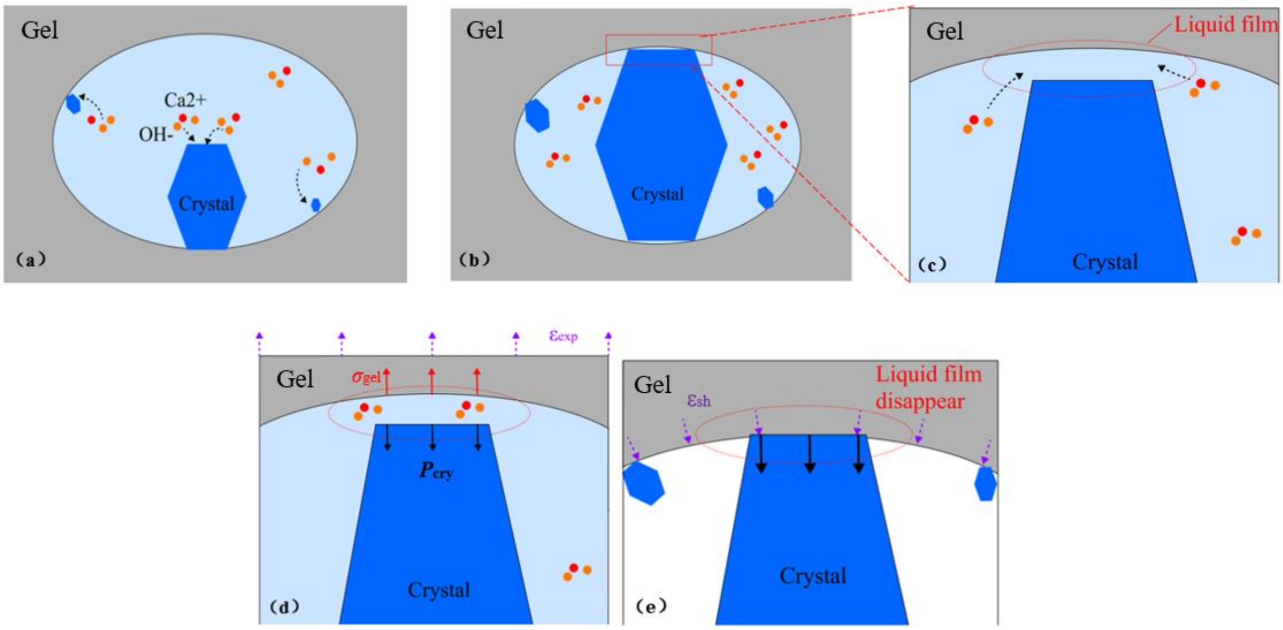

Fig. 1. The interactions between crystal and gel products in cement paste.

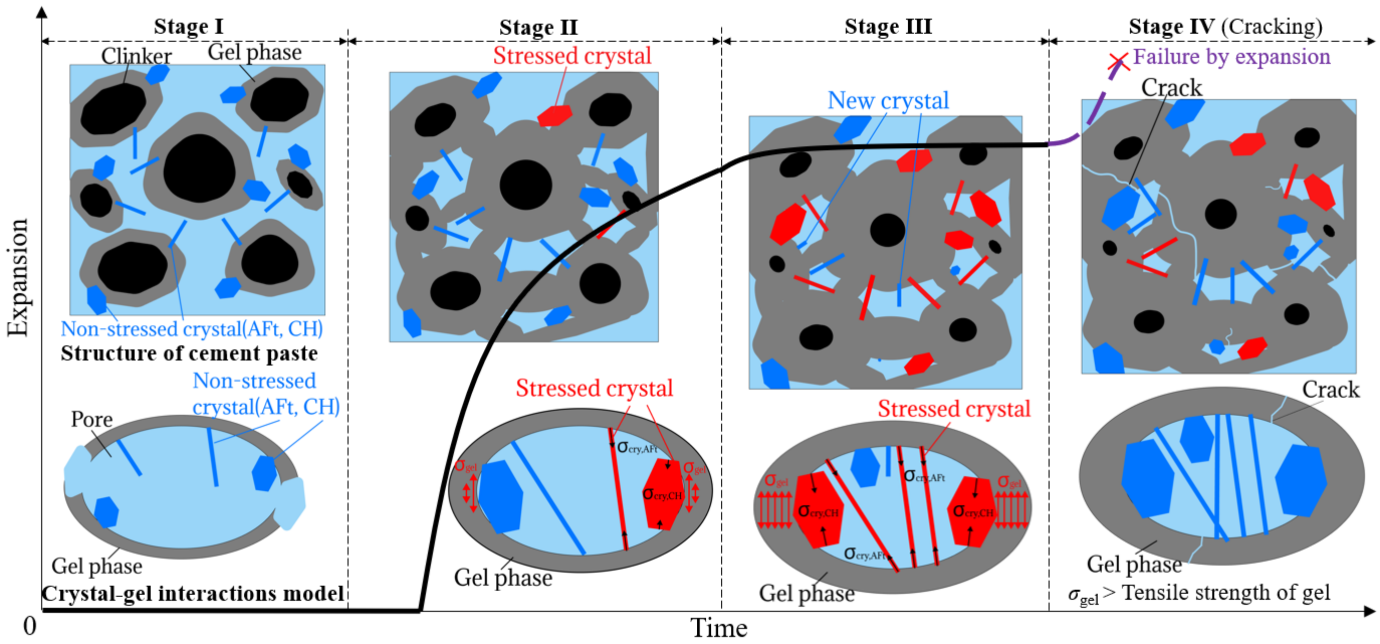

Fig. 2. Simplified model of volume change and microstructural development of cementitious materials.

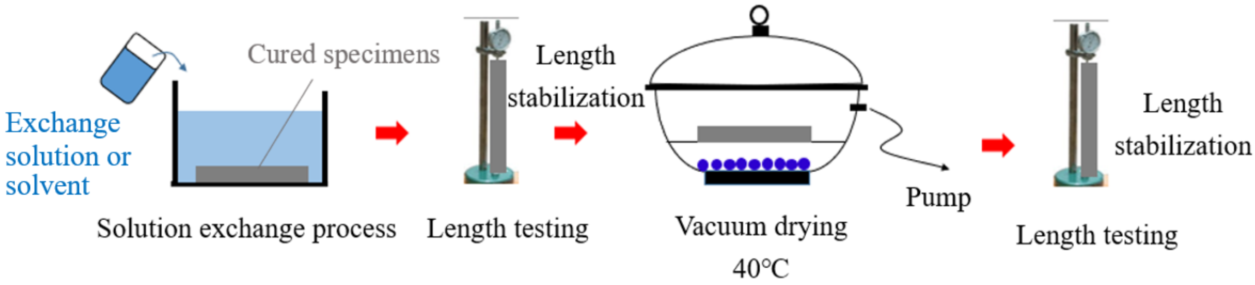

Fig. 3. Solvent/solution exchange and vacuum drying processes.

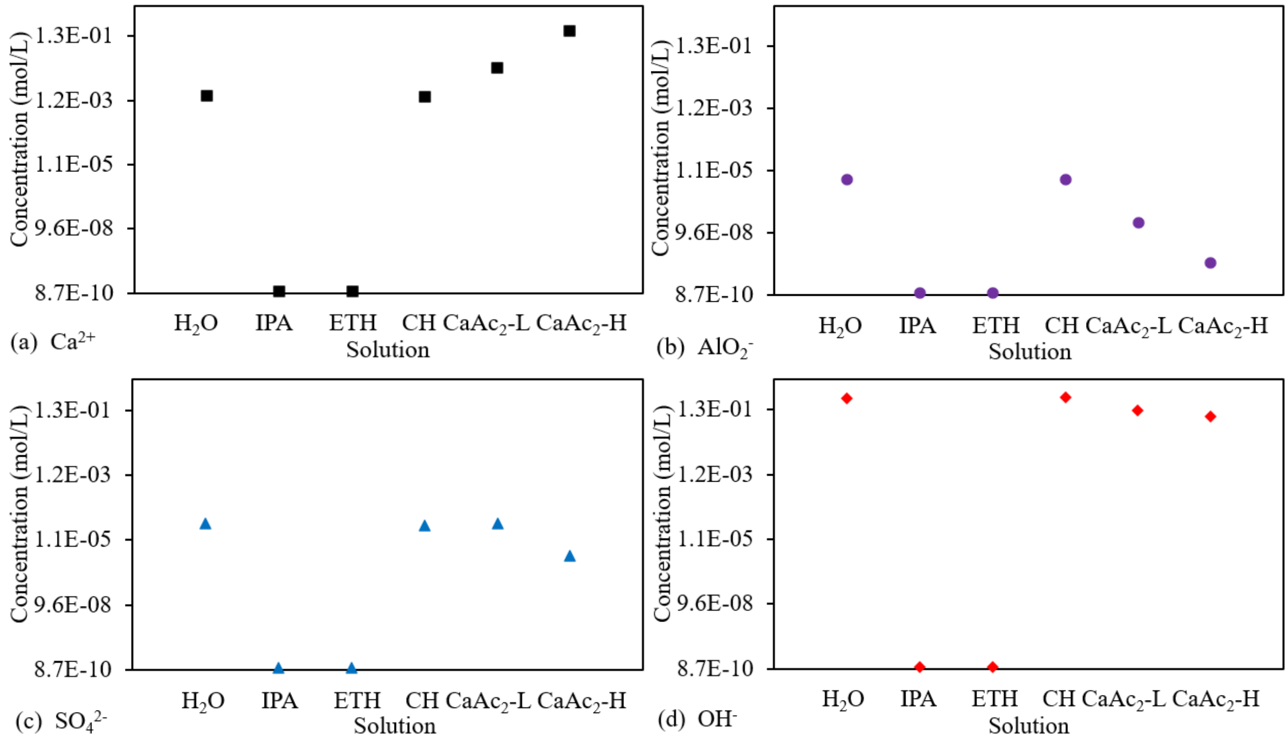

Fig. 4. Concentrations of Ca^{2+}, AlO_2^-, SO_4^{2-} and OH^- in different solvents and solutions (H_2O-water, IPA-isopropyl alcohol, ETH-ethanol, CH-calcium hydroxide, $CaAc_2$-calcium acetate, L-low concentration, H-high concentration).

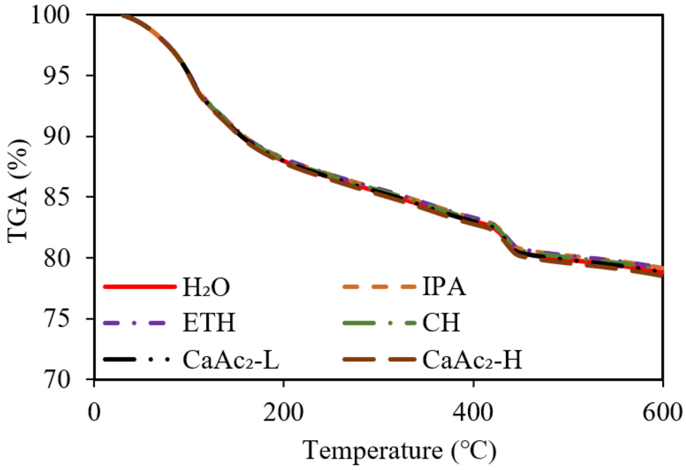

Fig. 5. TGA curves obtained for cement pastes immersed in different pore solvents or solutions (H_2O-water, IPA-isopropyl alcohol, ETH-ethanol, CH-calcium hydroxide, $CaAc_2$-calcium acetate, L-low concentration, H-high concentration).

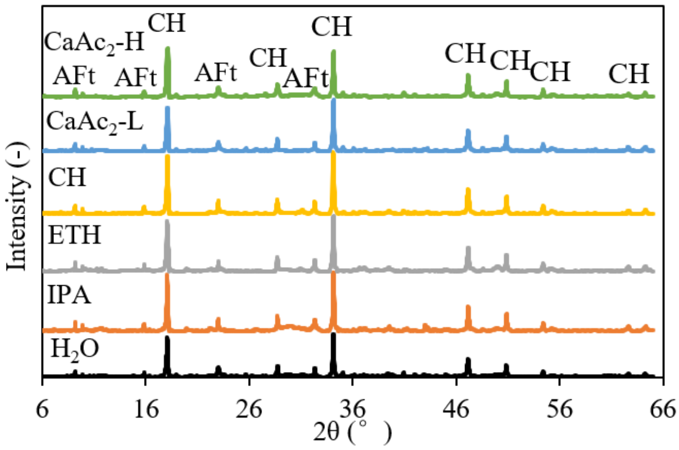

Fig. 6. XRD patterns obtained for cement pastes immersed in different pore solvents or solutions (H_2O-water, IPA-isopropyl alcohol, ETH-ethanol, CH-calcium hydroxide, $CaAc_2$-calcium acetate, L-low concentration, H-high concentration).

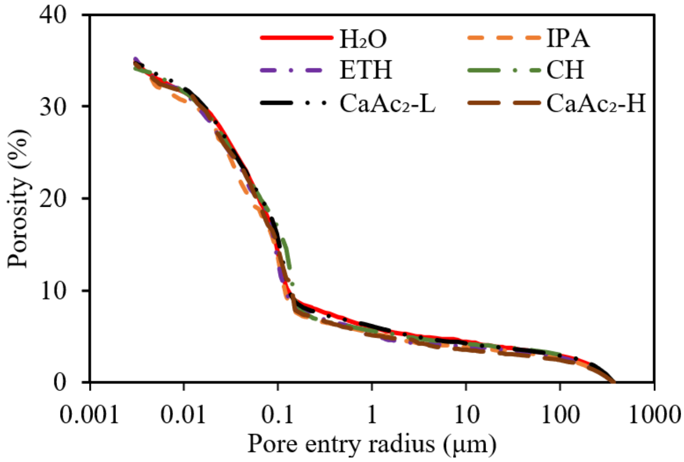

Fig. 7. Pore size distribution of cement pastes immersed in different pore solvents or solutions obtained from MIP tests (H_2O-water, IPA-isopropyl alcohol, ETH-ethanol, CH-calcium hydroxide, $CaAc_2$-calcium acetate, L-low concentration, H-high concentration).

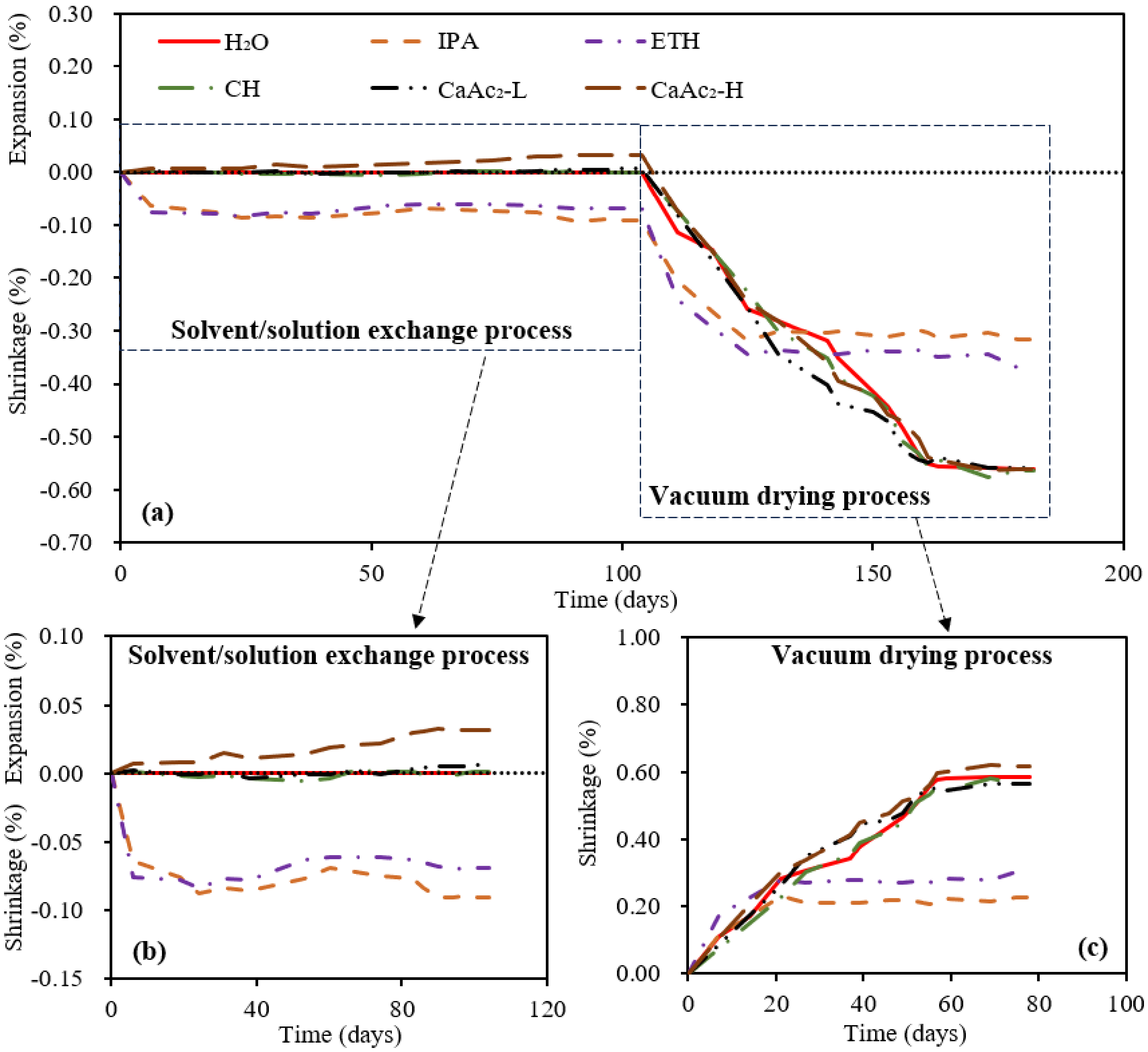

Fig. 8. (a) Length change of specimens throughout the whole process, (b) length change of specimens during solvent/solution exchange process and (c) length change of specimens during vacuum drying process (H_2O-water, IPA-isopropyl alcohol, ETH-ethanol, CH-calcium hydroxide, $CaAc_2$-calcium acetate, L-low concentration, H-high concentration).

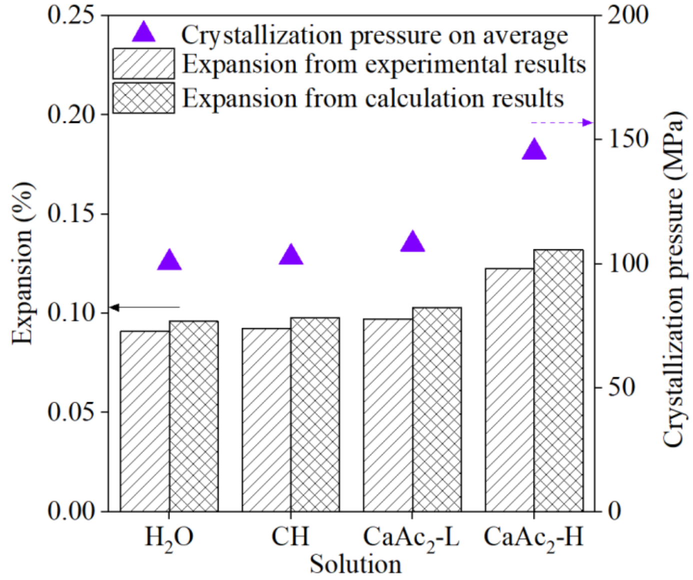

Fig. 9. Expansion of cement pastes within different crystallization pressures (H_2O-water, CH-calcium hydroxide, $CaAc_2$-calcium acetate, L-low concentration, H-high concentration).

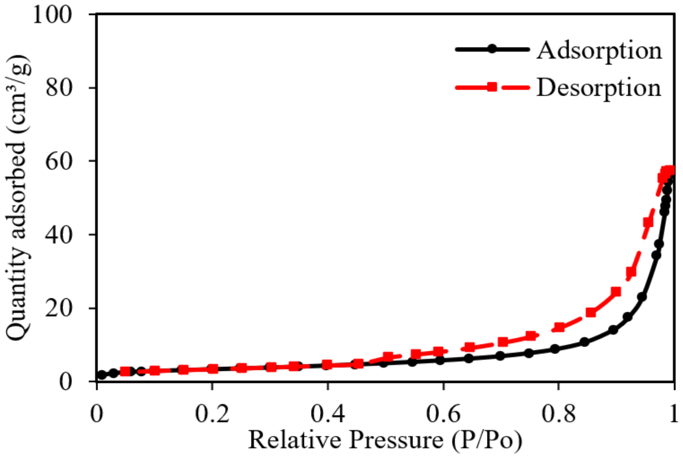

Fig. 10. Isothermal adsorption-desorption curve of the cement paste.

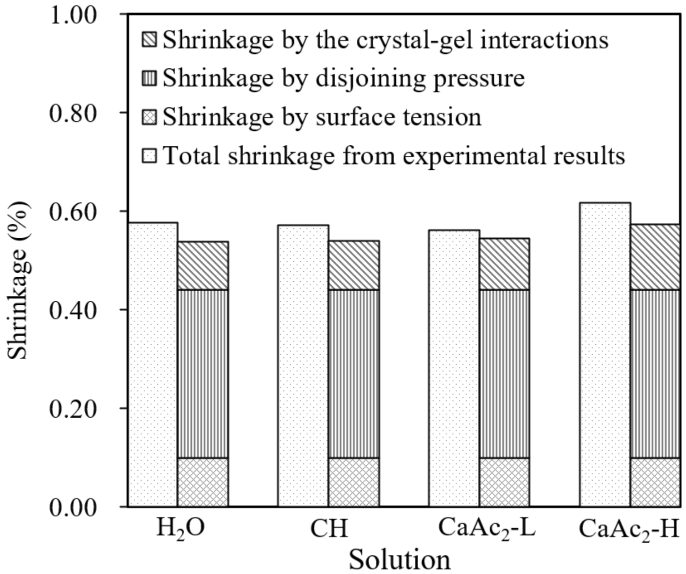

Fig. 11. Drying shrinkage of cement pastes (H_2O-water, CH-calcium hydroxide, $CaAc_2$-calcium acetate, L-low concentration, H-high concentration).

Table 1 RH ranges for the three mechanisms responsible for volume change of cement paste.

Mechanisms	Capillary forces	Solid surface tension	Disjoining pressure
RH	45%–100%	0–100%	0–45%

Table 2 Chemical composition of the Portland cement.

Composition	SiO_2	Al_2O_3	Fe_2O_3	CaO	MgO	SO_3
Content (wt.%)	20.85	5.28	2.54	61.64	2.58	2.06

Table 3 Properties of solvents and solutions.

Code	Solvent and solution	Concentration (g/100g water)	Concentration of Ca^{2+} (mol/L)	Concentration of OH^- (mol/L)
H_2O	Water	-	-	-
IPA	Isopropyl alcohol	Pure	-	-
ETH	Ethanol	Pure	-	-
CH	Calcium hydroxide	0.166 (saturated)	0.0224	0.0448
$CaAc_2$-L	Calcium acetate	0.354	0.0224	-
$CaAc_2$-H	Calcium acetate	3.54	0.224	-

Table 4 Types and contents of hydration products in cement paste.

Phase	C-S-H	CH	AFt	AFm
Content (wt.%)	44.76	22.15	6.59	3.98

Table 5 Average crystallization pressure for different cement pastes.

Code	H_2O	IPA	ETH	CH	$CaAc_2$-L	$CaAc_2$-H
Average crystallization pressure (MPa)	101.7	0	0	104.0	109.3	147.8

(H_2O-water, IPA-isopropyl alcohol, ETH-ethanol, CH-calcium hydroxide, $CaAc_2$- calcium acetate, L-low concentration, H-high concentration)